Accepted Manuscript

Sol-gel derived aluminium doped zinc oxide thin films: A view of aluminium doping effect on physicochemical and NO_2 sensing properties

A.R. Nimbalkar, N.B. Patil, V.V. Ganbavle, S.V. Mohite, K.V. Madhale, M.G. Patil

PII: S0925-8388(18)33816-7

DOI: 10.1016/j.jallcom.2018.10.144

Reference: JALCOM 47962

To appear in: *Journal of Alloys and Compounds*

Received Date: 28 August 2018

Revised Date: 11 October 2018

Accepted Date: 12 October 2018

Please cite this article as: A.R. Nimbalkar, N.B. Patil, V.V. Ganbavle, S.V. Mohite, K.V. Madhale, M.G. Patil, Sol-gel derived aluminium doped zinc oxide thin films: A view of aluminium doping effect on physicochemical and NO_2 sensing properties, *Journal of Alloys and Compounds* (2018), doi: https://doi.org/10.1016/j.jallcom.2018.10.144.

This is a PDF file of an unedited manuscript that has been accepted for publication. As a service to our customers we are providing this early version of the manuscript. The manuscript will undergo copyediting, typesetting, and review of the resulting proof before it is published in its final form. Please note that during the production process errors may be discovered which could affect the content, and all legal disclaimers that apply to the journal pertain.

Signature Not Verified
SHAHAJAHAN MEHABUB MANER
Document Certified

PDF SIGNER DEMO VERSION

Graphical Abstract

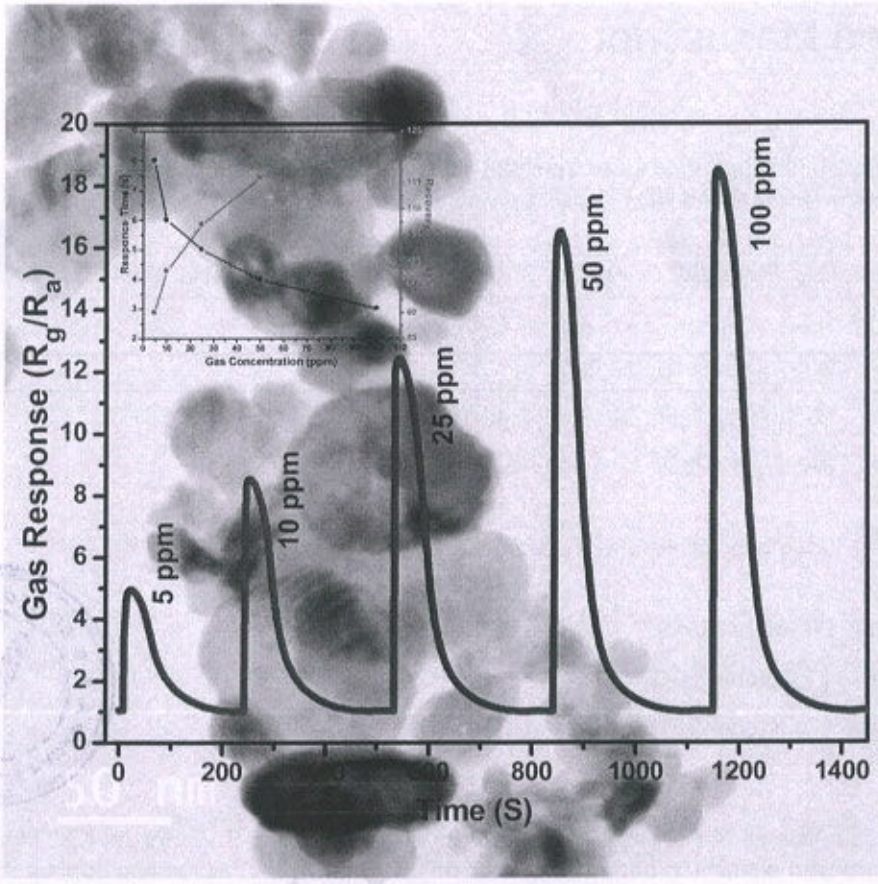

Signature Not Verified
SHAHAJAHAN MEHABUB MANER
Document Certified

ACCEPTED MANUSCRIPT

Sol-gel derived aluminium doped zinc oxide thin films: A view of aluminium doping effect on physicochemical and NO_2 sensing properties

A. R. Nimbalkar[a], N. B. Patil[b], V. V. Ganbavle[a], S.V. Mohite[c], K. V. Madhale[d], M. G. Patil[a]*

a Department of Physics, DKASC, Ichalkaranji, Maharashtra, India.

b SIT Polytechnic, Yadrav, Ichalkaranji, Maharashtra, India.

c Electrochemical Materials Laboratory, Department of Physics, Shivaji University, Kolhapur, Maharashtra, India

d Department of Physics, Walchand college of Engineering, Sangli, Maharashtra, India.

*** Corresponding Author at:** *E-mail address:* marutipatil1956@gmail.com

Fax: +91-230-2424555; Tel: +91-230-2420412.

Abstract

Aluminium doped ZnO (AZO) thin films have been synthesized by using a sol-gel spin coating method. The effect of Al-doping on physicochemical and NO_2 sensing properties of the AZO thin films were studied. The structural and compositional analysis confirms the phase formation of ZnO and substitution of aluminium atoms into zinc oxide lattice. The gas sensing performance of AZO thin films investigated at different operational temperatures towards NO_2 gas. The NO_2 sensing study reveals that the 2 at% AZO film sensor shows excellent gas sensing characteristics at 200°C.

Keywords: NO_2 gas; Selectivity; Sensors; Reproducibility; Thin films.

Signature Not Verified
SHAHAJAHAN MEHABUB MANER
Document Certified

ACCEPTED MANUSCRIPT

1. Introduction

Normally the resistance of a sensor based on oxide material film varies in the environment of various oxidizing or reducing gases. Because of that, oxide films gained an additional attraction towards gas detection application in a sensor field [1]. In various oxides materials, zinc oxide (ZnO) is a graceful material due to its morphological diversity, higher sensitivity, selectivity with very good durability towards detection of various noxious and volatile gases [2]. Several synthesis methods used for deposition of ZnO films such as sol-gel, CBD, RF magnetron sputtering, PLD, spray pyrolysis, SILAR, and hydrothermal method [3-10]. The economical sol-gel spin coating method used in this work. The process in sol-gel spin coating method is straightforward and the deposition takes place at a room temperature. The sensors based on zinc oxide have been broadly studied to detect various noxious and volatile gases viz. methanol, ethanol, acetone, H_2, LPG, NH_3, CO, H_2S, and NO_2 [11–18]. Using an appropriate dopant material in ZnO like Al, Co, Sn, Ru, In, Cu, Fe, Ga etc. improves sensors gas detection capability [19]. The dopant material creates various electronic defects in sensor films, which improve the effect of partial pressure of oxygen species on sensor conductivity [20]. The doped aluminium plays a crucial role in zinc oxide film based gas sensors. Because, doped Al enhances the gas sensing characteristics by varying the ZnO energy band structure and amplifies the interaction of gas molecules on the sensor surface by enhancing the surface-volume ratio of sensor film [21].

NO_2 is a very noxious gas, mostly generated from various anthropogenic and natural sources; such as volcanic activity, plants, heaters, combustion engines, furnaces and generation of electricity [22]. NO_2 gas is one of the highly noxious and injurious at its lower concentration level to not only human health but also all living organisms [23].

Signature Not Verified
SHAHAJAHAN MEHABUB MANER
Document Certified

ACCEPTED MANUSCRIPT

Accordingly, the synthesis of a sensor to detect NO_2 gas molecules at a lower level concentration with excellent gas sensing characteristics are required [23].

Nowadays, studies conducted to improve the properties of films by modifying the structural, electrical, optical, development of defects and enhanced gas sensing by doping different metal elements in ZnO thin films. For detection of different noxious gases, various researchers studied pure and doped ZnO thin film based sensors [25]. It is well known that the very less amount of doping of Al atoms in the ZnO film will modify the electrical conductivity [25]. Therefore, we attempt to prepare Al-doped ZnO (AZO) thin films for detection of NO_2 gas molecules at a lower level concentration. We reported on the very much selective and sensitive AZO sensor film towards NO_2, prepared by an uncomplicated sol-gel spin coating method. The difference in a physicochemical and NO_2 gas detection characteristics because of the aluminium doping are investigated as a function of doping concentration (0–4 at%).

2. Experimental procedure

The ZnO thin film was deposited by a sol-gel spin coating method on a glass substrate, as reported previously [24]. Similarly, synthesis AZO thin films were done at 1–4 at% (atomic weight %) doping concentration. Then the prepared thin films annealed in air ambient at 400°C for 2 h. Thus, in this study, we attempt to improve structural and morphological properties to enhance NO_2 sensing performance by doping Al in ZnO thin films.

The following characterizations tools used for investigation physicochemical properties: XRD (Bruker D2 phaser), XPS (XPSPHI, 5000 Versa Probe II USA),

Signature Not Verified
SHAHAJAHAN MEHABUB MANER
Document Certified

ACCEPTED MANUSCRIPT

FESEM (Zeiss Ultra, 55 FE-SEM), HRTEM (Tecnai G2 F30, FEI), Bruker Dektakxt profilometer used to measure thickness of AZO films.

The gas detection studies of synthesized AZO films based on the difference in resistance, in analyte test gas ambient, the resistance of sensor was measured and recorded in air ambient and existences of NO_2 gas molecules by using a locally designed two-probe gas sensing unit connected to the Keithley electrometer 6514 model USA. For NO_2 sensing studies, the sensor film placed in the sealed test chamber and the analyte test gas inserted in the test chamber of a sensing unit at 100–300°C operational temperature range. The sensor resistance in the absence (R_a) and in the occurrence of analyte test gas (R_g) measured and recorded to determine the gas response R_s, defined as follows: $R_s = R_g / R_a$.

3. Results and discussion

The XRD patterns of the AZO films in the 2θ range of 10 – 90^0 shows in Fig. 1. The patterns show well-defined and aculeate peaks, all diffraction peaks and lattice parameters are in fine arrangement with a wurtzite structure (JCPDS card No. 01-079-0205). No other extra peaks detected, which ascribed to the impurities, which accentuate the higher degree of purity with a phase of the as-synthesized AZO thin films. The (0 0 2) plane peak intensity is enormous than the other peaks, which shows that the AZO films oriented along c-axis and grown precisely with the (0 0 2) plane, which suggests an excellent quality of films and nonexistence of a secondary phase formation in the AZO films [19]. The (0 0 2) plane peak intensity increases with increasing aluminium doping concentrations (0–2 at%), but after that reduces for higher aluminium doping concentrations level (3–4 at%). The variation in (0 0 2) plane peak

Signature Not Verified
SHAHAJAHAN MEHABUB MANER
Document Certified

ACCEPTED MANUSCRIPT

intensity confirms the incorporation of Al atoms into ZnO lattice, without changing their wurtzite structure in accordance with the earlier studies [25]. XRD peaks intensities decreases at higher Al-doping concentration because of the defect states generated by Al dopant atoms. The crystallite size is calculated by using a Debye-Scherrer formula [26]. The average crystallite size and lattice constant of AZO thin films from the XRD pattern represented in Table no.1. From XRD study, no considerable variation in the crystallite size is observed in AZO films.

The compositional and valence states of elements on the surface of the synthesized AZO thin films examine by using an XPS spectroscopy. XPS survey scan spectrum of AZO thin films represented in Fig. 2 (a), which confirms the existences of Zn, Al, O and C elemental species in synthesized films, which displays the high degree of purity of synthesized films. The impurity peaks are not observed attributed to other elements in synthesized films. The C 1s peak used as a reference in the XPS spectrum of binding energy 283.26 eV [27]. A very small shifting for Zn and O elements peak positions are observed due to the Al-doping, which reveals the unchanged Zn chemical state after Al-doping. Standard [28] and detected peak positions of different elements existed in dissimilar structures of synthesized films are tabulate in Table 2. The values in Table 2 confirm the existed elements peak positions are in fine-agreement with the past reported values [28]. Fig. 2 (b) shows the Zn 2p narrow scan spectrum. The Zn $2p_{3/2}$ and Zn $2p_{1/2}$ splitting of the Zn 2p doublet are 23.01 eV, 23.10 eV, 23.15 eV, 23.06 eV, 23.03 eV observed for 0–4 at% AZO films respectively [28] and validates the oxidized state of Zn element. The 2p peak intensity rises with increasing Al-doping concentration up to the 2 at% and then reduces at higher 3–4 at% Al-doping

S. C. COLLEGE ICHALKARANJI

Signature Not Verified
SHAHAJAHAN MEHABUB MANER
Document Certified

concentration. The incorporation of Al atoms into ZnO lattice is effectual up to 2 at% but at higher doping levels, Al atoms remain as a defect levels [29].

The O 1s peaks of AZO thin films represented in Fig.2 (c). The O 1s peak of B.E. centres at 529.81 eV, 530.15 eV, 530.04 eV, 530.02 eV and 529.98 eV for 0–4 at% AZO film, respectively. The centre of peaks at 530 eV corresponds to the oxygen species at O 1s core level and Zn^{2+} ions of the ZnO [29, 30]. Fig. 2 (d) shows the narrow scan of Al 2p. The B.E of a peak at about 73 eV attributed to Al 2p, which confirms the incorporation of Al atoms into ZnO lattice [31]. The Al 2p peaks intensity increases with increasing Al-doping from 1 to 4 at%. The variation in peak intensity and position in XRD pattern and in XPS spectra with Al-doping are observed, which confirms the doping of Al atoms into ZnO lattice.

Fig. 3 shows the FESEM images of AZO thin films. The morphology of films examined from 2-D FESEM images; it shown that the synthesized films are made-up of consistent spherical crystallites with a number of pores. The synthesized films with porous characteristic consisting of AZO nanoparticles in ~35 nm diameters range. The porous structured surface morphology offers a superior sensing area for the diffusion of test gas molecules, which enhances the rate of reaction among the gas molecules and sensor surface, which enhance the sensitivity of the sensor [32]. The existences of doping atoms in a host material modify the relative energy of the crystal faces; therefore, observe the variation in a host material morphology [33]. The substitution of Al atoms for Zn sites increases the nucleation sites on the surface of substrate [24, 34]. The slightly difference in surface morphology of AZO films are observed. The FESEM image of 2 at% AZO film shows the cluster of small nanocrystallites. The small

DATTAJIRAO KADAM A. S. C. COLLEGE, ICHALKARANJI ICHALKARANJI

Signature Not Verified
SHAHAJAHAN
MEHABUB MANER
Document Certified

ACCEPTED MANUSCRIPT

nanocrystallites in 2 at% AZO film enhances the sensing surface area of sensor film than the other AZO films, which is excellent for gas detection [35].

Fig. 4 represents the TEM, HRTEM and SAED images of the pure and 2 at% AZO crystallites with well-resolved lattice fringes and crystalline nature. The TEM images [Fig. 4 (a, b, d, and e)] shows spherical shaped crystallites aggregated with smaller crystallites, which creates various diffusion sites for gas adsorption. Fig. 4 (d and e) reveals the crystallites shape remains unchanged after Al-doping. Fig. 4 (c and f) represents the HRTEM images of the ZnO and 2 at% AZO crystallites, which shows clear and sharp lattice fringes. The interplanar spacing (d) among the two parallel fringes is around 0.26 nm for both ZnO and 2 at% AZO crystallites and similar to the interplanar spacing (d) value determined from the XRD analysis for (0 0 2) plane. Inset of Fig. 4 (b and e) represents SAED pattern of pure and 2 at% AZO crystallites. The intense diffraction spots exhibit the high-degree of ZnO and AZO crystallites with wurtzite structure. These intense spots arranged in six concentric rings attributed to the plane found in XRD analysis, which confirms the wurtzite structure of crystallites in synthesized films.

The electrical conductivity study of synthesized AZO films performed at 300–573K temperature range by using a two-probe method. The variation in electrical conductivity (σ) regarding temperature for AZO films shows in Fig.5. The electrical conductivity of AZO films increases from 10^{-7} to 10^{-4} S/cm with increasing temperature reveals the semiconducting behavior of AZO films [36]. The plot of ln σ versus 1000/T for AZO films represents in the inset of Fig.5. The activation energy calculated from the slope of the ln σ versus 1000/T curve using the following formula:

$$\sigma = \sigma_o \exp(-E_a/KT) \qquad (1)$$

Signature Not Verified
SHAHAJAHAN
MEHABUB MANER
Document Certified

Where, E_a = activation energy, σ_o = proportionality constant, K = Boltzmann constant and T = temperature [37]. The activation energy of synthesized AZO thin films has been reduces with increasing Al-doping concentration from 0.45 eV to 0.39 eV. The activation energy of AZO films reveals the excitation of thermally activated electrons from donor levels to the conduction band, due to amplified temperature [38].

The NO_2 sensing studies of AZO thin films examined as a function of analyte test gas concentration with respect to the time. To find out the optimized operational temperature of sensor film, NO_2 sensing studies performed at 100–300°C temperatures range at a fixed gas concentration (100 ppm). Inset of the Fig. 6 represents the NO_2 response of AZO films at 100 ppm gas concentration in the temperatures range of 100–300°C. The 2 at% AZO film shows an enhanced NO_2 response at 200°C than the other films. Inset of the Fig. 6 shows the AZO films gas response is staidly enhances up to 200°C and reduces at higher (>200°C) temperature. At lower (<200°C) temperature the sensor response is less due to a slow rate of chemical reaction (adsorption and desorption) among the sensor surface and test gas. But, at higher (>200°C) temperature sensor response is less because the elevated rate of desorption reaction than the rate of adsorption reaction of test gas molecules with the sensing layer. At optimum temperature (200°C) the rate of adsorption and desorption reactions become equivalent, then sensor shows highest NO_2 response [39]. The 200°C working temperature is beneficial because the warm-up time require for a sensor is small and it decreases drift in the signals that takes place because of conversion of small grains to the large grains upon constant heating of the sensor [40]. The response curves of the AZO thin films towards NO_2 gas at 100 ppm concentration at 200°C represented in the Fig. 6. Among them, 2 at% AZO sensor film shows an elevated response that's why 2 at% Al-doping

Signature Not Verified
SHAHAJAHAN
MEHABUB MANER
Document Certified

ACCEPTED MANUSCRIPT

concentration consider as optimum doping level. The NO_2 response enhances with increasing concentration of Al-doping up to 2 at% and then reduces at higher Al-doping concentration. This is because of the cluster of small nanocrystallites in 2 at% AZO film as observed in FESEM study, which increases sensing surface area of sensor film. So, for further investigation of response of 2 at% AZO film towards various NO_2 gas concentrations are measured and recorded at 200°C.

The 2 at% AZO sensor response towards various gas concentrations measured to find out the smaller amount of sensing limit towards NO_2 gas. The difference in the sensor resistance in the ambient of NO_2 gas molecules measured and recorded at 200°C towards 5–100 ppm concentration. Fig.7 shows the resistance of sensor rises from the initial resistance after NO_2 exposure and attains the highest value in a very short time and after that gradually reduces after introduce the fresh air. The variation in resistance of sensor film is as a result of the reactions among the analyte test gas molecules and porous sensing layer of sensor. Fig. 8 shows the 2 at% AZO sensor response towards different NO_2 concentration at 200°C, which indicates that the 2 at% AZO sensor response enhances with amplifying the gas molecules concentration and shows an analogous performance for higher (>5 ppm) concentrations. The 2 at% AZO sensor response enhanced from 5.0 to 18.5 for 5 ppm to 100 ppm NO_2 gas, respectively. The least sensing limit of NO_2 gas molecules accomplished for 5 ppm but it shows the lowest gas response. At lower concentration level test gas molecules covers very less sensing area on a sensing layer causes very slow chemical reaction rate on a sensor surface. But at higher NO_2 gas molecules (100 ppm) concentration it shows the highest response because at higher concentration level test gas molecules covers the more sensing area on sensing layer then the rate of a chemical reaction is enhances [39]. The

Signature Not Verified
SHAHAJAHAN
MEHABUB MANER
Document Certified

observed NO_2 sensing characteristics compared with other sensors synthesized by various methods, shown in Table 3.

The sensing mechanism of sensor materials involves two key reactions: adsorption and desorption of O_2^-, O^- and O^{2-} species on a sensing layer of sensor. The absorbed oxygen species trap the electrons from the conductance band plays a vital role in gas detection [41], because these reactions causes a variation in the sensor resistance [42]. Inset of the Fig. 8 shows the variation in response/recovery time of 2 at% AZO sensor with various gas concentrations. The response/recovery times calculated from the variation in gas response with time towards 5–100 ppm concentration. From the figure, both terms vary contrariwise with a concentration of NO_2 gas molecules. The response time reduces from 14 to 8 s but recovery time goes up from 90 to 121 s towards 5 ppm to 100 ppm NO_2 gas. The response time reduces because of the various empty sites on the sensor layer for the gas adsorption and the amplification in recovery time because of the chemisorption of various oxygen species on the sensor layer and it wants an extensive period intended for total desorption of gas molecules. For convenient dependability of a sensor material is depends on the reproducibility showed by the sensor. The reproducibility property of 2 at% AZO sensor is examined by performing sensing test for four times at 200°C at constant NO_2 (100 ppm) concentration. Fig.9 revealed that the response of the 2 at% AZO sensor towards NO_2 gas is constant for each sensing test, which confirms the reproducibility of sensor material. The selectivity of 2 at% AZO sensor investigated at 200°C, towards various analyte gases viz. NH_3, CH_3OH, LPG, C_2H_5OH, H_2S, Cl_2 and NO_2 at a constant concentration (100 ppm). Fig.10 reveals that the 2 at% AZO sensor film is selective with highest gas response for NO_2 than the different analyte test gases, attributed to the

Signature Not Verified
SHAHAJAHAN
MEHABUB MANER
Document Certified

superior reactivity of NO_2 gas molecules with the sensor surface [24]. Selectivity coefficient (K) of NO_2 gas regarding other gases calculated by using the following relation and represented in Table 4.

$$K = |S_a/S_b| \qquad (2)$$

Where, S_a = NO_2 response and S_b = response towards other gases. Table 5 reveals the NO_2 response of 2 at% AZO sensor film is the 4.8–18.3 times higher than the other gases for equivalent gas concentration. A higher selectivity and response towards NO_2 in the existences of various gases recommends utilization of 2 at% AZO sensor material for NO_2 detection.

4. Conclusions

Aluminium doped zinc oxide (AZO) thin films effectively synthesized by a sol-gel spin coating method. The doping of a small amount of aluminium (Al) slightly changes the structural, chemical, morphological and electrical properties of AZO films. The 2 at% AZO film shows spherical porous structured nanocrystallites aggregated with small nanocrystallites creates various active sites for adsorption of gas molecules. The conductivity study reveals that the activation energy of the AZO films has been decreases with increasing Al doping concentration. The NO_2 sensing properties of the AZO thin films at different Al-doping concentration carried out at various operational temperatures. The 2 at% AZO thin film shows the enhanced response towards NO_2 gas at 200°C. From gas sensing performance of synthesized films, it is concluded that, the 2 at% AZO thin film having excellent NO_2 sensing characteristics such as higher gas response (18.5), fast response/recovery times, admirable reproducibility at 200°C and also capable to sense lower concentration (5 ppm) with a good response value. These

Signature Not Verified
SHAHAJAHAN
MEHABUB MANER
Document Certified

results indicate that the 2 at% AZO thin film can stand as an excellent sensing material for NO_2 detection.

Acknowledgements

The authors are thankful to the center of Excellence in Nano-electronics (CEN) at Indian Institute of technology, Bombay under Indian Nanoelectronics User Program (INUP) for providing characterization facility.

References

[1] S. G. Pawar, S. L. Patil, M. A. Chougule, B. T. Raut, S. A. Pawar, R. N. Mulik, V. B. Patil, J Mater Sci.: Mater Electron 23 (2012) 273–279.

[2] N. Tamaekong, C. Liewhiran, A. Wisitsoraat, A. Tuantranont, S. Phanichphantd, Sensors and Actuators B 204 (2014) 239–249.

[3] Amol R. Nimbalkar, Maruti G. Patil, Physica B 527 (2017) 7–15.

[4] Alex M. Ma, Manisha Gupta, Fatema Rezwana Chowdhury, Mei Shen, Kyle Bothe, Karthik Shankar,Ying Tsui, Douglas W. Barlage, Solid-State Electronics 76 (2012) 104–108.

[5] O. Lupan, T. Pauporte´, L. Chow, B. Viana, F. Pelle´, L. K. Ono, B. Roldan Cuenya, H. Heinrich, Applied Surface Science 256 (2010) 1895–1907.

[6] Said Benramachea, Achour Rahalb, Boubaker Benhaoua, Optik 125 (2014) 663–666.

[7] C. Y. Kung, C. C. Lin, S. L. Young, Lance Horng, Y. T. Shih, M. C. Kao, H. Z. Chen, H. H. Lin, J. H. Lin, S. J. Wang, J. M. Li, Thin Solid Films 529 (2013) 181–184.

Signature Not Verified
SHAHAJAHAN
MEHABUB MANER
Document Certified

ACCEPTED MANUSCRIPT

[31] Venkateswarlu Gaddam, R. Rakesh Kumar, Mitesh Parmar, G R Krishna Yaddanapudi, M.M.Nayak and K.Rajanna, RSC Adv., 5 (2015) 13519-13524.

[32] S. T. Navale, A. T. Mane, M. A. Chougule, R. D. Sakhare, S. R. Nalage, V. B. Patil Synthetic Metals 189 (2014) 94– 99.

[33] V. V. Ganbavle, S. K. Patil, S. I. Inamdar, S. S. Shinde, K. Y. Rajpure, Sensors and Actuators A 216 (2014) 328–334.

[34] Amol R. Nimbalkar, Maruti G. Patil, Materials Science in Semiconductor Processing 71 (2017) 332–341.

[35] Trilochan Sahoo, Myoung Kim, Mi-Hee Lee, Lee-Woon Jang, Ju-Won Jeon, Joon Seop Kwak, In-Yong Ko, In-Hwan Lee, Journal of Alloys and Compounds 491 (2010) 308–313.

[36] S. R. Aghdaee, V. Soleimanian, B. Tayebi, Superlattices and Microstructures 51 (2012) 149–162.

[37] Yasin Sahin, Sadullah Öztürk, Necmettin Kılınc, Arif Kösemen, Mustafa Erkovan, Zafer Ziya Öztürk, Appl. Surf. Sci. 303 (2014) 90–96.

[38] Yasemin Caglar, Müjdat Caglar, Saliha Ilican, Current Applied Physics 12 (2012) 963–968.

[39] A. T. Mane, S. B. Kulkarni, S. T. Navale, A. A. Ghanwat, N. M. Shinde, JunHo Kim, V. B. Patil, Ceramics International 40 (2014) 16495–16502.

[40] G. Eranna, B. C. Joshi, D. P. Runthala, and R. P. Gupta, Critical Reviews in Solid State and Materials Sciences 29 (2004) 111–188.

[41] K. Arshak, I. Gaidan, Materials Science and Engineering B 118 (2005) 44–49.

[42] S. Öztürk, N. Kılınç, N. Taşaltin, Z.Z. Öztürk, nanowires and nanorods, Thin Solid Films 520 (2011) 932–938.

DATTAJIRAO KADAM A. S. C. COLLEGE ICHALKARANJI

Signature Not Verified
SHAHAJAHAN MEHABUB MANER
Document Certified

ACCEPTED MANUSCRIPT

Figure captions

Figure 1 XRD pattern of AZO thin films.

Figure 2 (a) Survey scan (b) narrow scan of Zn 2p doublet (c) narrow scan O 1s core level (d) narrow scan of Al 2p core level of AZO thin films.

Figure 3 FESEM images for AZO thin films: (a) ZnO, (b) 1 at% AZO and (c) 2 at% AZO (d) 3 at% AZO (e) 4 at% AZO.

Figure 4 TEM, HRTEM and SAED images of ZnO and 2 at% AZO thin film.

Figure 5 Plot of dc-conductivity with temperature and inset shows lnσ versus 1000/T of AZO thin films.

Figure 6 Response of AZO thin films at 200°C and inset shows response at different operating temperature.

Figure 7 Electrical response of 2 at% AZO sensor film with time towards NO2 gas.

Figure 8 Dynamic gas response and inset shows response/recovery time of 2 at% AZO sensor film.

Figure 9 Reproducibility of 2 at% AZO sensor film.

Figure 10 Selectivity studies of 2 at% AZO thin film.

Table caption

Table 1 Values of various parameters calculated from XRD.

Table 2 The B. E. positions of the element present in different structures of ZnO.

Table 3 Comparison of NO_2 sensing properties of sensors synthesized by various methods.

Table 4 selectivity coefficient (K) of 2 at% AZO thin film.

Signature Not Verified
SHAHAJAHAN
MEHABUB MANER
Document Certified

ACCEPTED MANUSCRIPT

[8] Arindam Ghosh, Ramphal Sharma, Anil Ghule, Vidya S. Taur, Rajesh A. Joshi, Dipalee J. Desale, Yuvraj G. Gudage, K. M. Jadhav, Sung-Hwan Han, Sensors and Actuators B 146 (2010) 69– 74.

[9] S. Kahraman, H. M. Cakmak, S. Cetinkaya, F. Bayansal, H. A. Cetinkara, H. S. Guder, Journal of Crystal Growth 363 (2013) 86–92.

[10] M. Vishwas, K. Narasimha Rao, A. R. Phani, K. V. Arjuna Gowda, R. P. S. Chakradhar, Solid State Communications 152 (2012) 324– 327.

[11] S. S. Nath, M. Choudhury, D. Chakdar, G. Gope, R. K. Nath, Sensors and Actuators B 148 (2010) 353–357.

[12] Muhammad Amin, Nazar Abbas Shah, Arshad Saleem Bhatti and Mohammad Azad Malik, Cryst. Eng. Comm. 16 (2014) 6080.

[13] Cuiping Gu, Jiarui Huanga, Youjie Wu, Muheng Zhai, Yufeng Sun, Jinhuai Liu, Journal of Alloys and Compounds 509 (2011) 4499–4504.

[14] Oleg Lupan, Lee Chow, Guangyu Chai, Sensors and Actuators B 141 (2009) 511–517.

[15] Hyung-Sik Woo, Chang-Hoon Kwak, Il-Doo Kim and Jong-Heun Lee, J. Mater. Chem. A 2 (2014) 6412.

[16] K. V. Gurav, V. J. Fulari, U. M. Patil, C. D. Lokhande, Oh-Shim Joo, Applied Surface Science 256 (2010) 2680–2685.

[17] R. Mariappan, V. Ponnuswamy, P. Suresh, N. Ashok, P. Jayamurugan, A. Chandra Bose, Superlattices and Microstructures 71 (2014) 238–249.

[18] Camelia Matei Ghimbeu, Joop Schoonman, Martine Lumbreras, Maryam Siadat, Applied Surface Science 253 (2007) 7483–7489.

[19] Satish S. Badadhe, I. S. Mulla, Sensors and Actuators B 143 (2009) 164–170.

DATTAJIRAO KADAM A. S. C. COLLEGE ICHALKARANJI

Signature Not Verified
SHAHAJAHAN
MEHABUB MANER
Document Certified

[20] S. D. Shinde, G. E. Patil, D. D. Kajale, V. B. Gaikwad, G. H. Jain, Journal of Alloys and Compounds 528 (2012) 109–114.

[21] Handan Aydın, Fahrettin Yakuphanoglu, Cihat Aydın, Journal of Alloys and Compounds 773 (2019) 802–811.

[22] M. Breedon, M. J. S. Spencer, I. Yarovsky, Surface Science 603 (2009) 3389–3399.

[23] Y. H. Navale, S. T. Navale, F. J. Stadler, N. S. Ramgir, A. K. Debnath, S. C. Gadkari, S. K. Gupta, D. K. Aswal, V. B. Patil, Ceramics International 43:9 (2017) 7057–7064.

[24] Nilam B. Patil, Amol R. Nimbalkar, Maruti G. Patil, Materials Science & Engineering B 227 (2018) 53–60.

[25] Pankaj S. Kolhe , Alpana B. Shinde, S.G. Kulkarni, Namita Maiti, Pankaj M. Koinkar, Kishor M. Sonawane, Journal of Alloys and Compounds 748 (2018) 6–11.

[26] H. Benelmadjat, N. Touka, B. Harieche, B. Boudine, O. Halimi, M. Sebais, Optical Materials 32 (2010) 764–767.

[27] Prabhakar Rai, Yun-Su Kim, Hyeon-Min Song, Min-Kyung Song, Yeon-Tae Yu, Sensors and Actuators B 165 (2012) 133–142.

[28] Leong G. Mar, Peter Y. Timbrell and Robert N. Lamb, Thin Solid Films 223 (1993) 341–347.

[29] V. V. Ganbavle, S. I. Inamdar, G. L. Agawane, J. H. Kim, K. Y. Rajpure, Chemical Engineering Journal 286 (2016) 36–47.

[30] J. Das, S. K. Pradhan, D. R. Sahu, D. K. Mishra, S. N. Sarangi, B. B. Nayak, S. Verma, B. K. Roul, Physica B 405 (2010) 2492–2497.

Signature Not Verified
SHAHAJAHAN
MEHABUB MANER
Document Certified

ACCEPTED MANUSCRIPT

Table 1

Samples	Film thickness (nm)	Lattice parameters (Å)	Average Crystallite size (nm)	Activation energy (eV)
ZnO	151	c = 5.19, a = 3.24	32	0.45
1 at% AZO	156	c =5.19, a = 3.24	34	0.43
2 at% AZO	163	c = 5.19, a = 3.24	35	0.42
3 at% AZO	158	c = 5.20, a = 3.25	33	0.41
4 at% AZO	161	c = 5.18, a = 3.24	35	0.39

Signature Not Verified
SHAHAJAHAN
MEHABUBMANER
Document Certified

ACCEPTED MANUSCRIPT

Table 2

Sr. No.	Chemical species	Observed BE (eV)					Standard BE (eV)
		ZnO	1 at% AZO	2 at% AZO	3 at% AZO	4 at% AZO	
1	C 1s	282.91	283.85	283.44	283.68	283.38	283.26
2	Zn $2p_{1/2}$	1044.08	1044.21	1044.19	1044.11	1044.12	1044.70
3	Zn $2p_{3/2}$	1021.07	1021.11	1021.04	1021.05	1021.09	1021.40
4	Zn 3s	138.05	138.23	138.21	138.00	137.94	139.40
5	O 1s	529.81	530.15	530.04	530.02	529.98	530.21
6	Al 2p	-	73.35	73.37	73.25	73.27	74.6

Signature Not Verified
SHAHAJAHAN
MEHABUBMANER
Document Certified

Table 3

Method of preparation	Materials	NO_2 Concentration (ppm) and Operating Temperature (°C)	Response	Response / recovery time (s)	Ref. no.
Spray pyrolysis	ZnO	1 / 300	1.84	- / -	18
Thermal evaporation	CuO	100 / 150	48%	11 / 550	22
Hydrothermal	ZnO	50 / 300	10	- / -	26
Spray pyrolysis	Ni:ZnO	100 / 200	108%	11 / 123	28
Sol-gel spin coating	PPy	100 / RT	36%	126 / 2170	31
Sol-gel drop casting	WO_3	100 / 200	34%	- / -	32
Sol-gel spin coating	Al:ZnO	100 / 200	18.5	8 / 121	this work

Signature Not Verified
SHAHAJAHAN
MEHABUB MANER
Document Certified

Table 4

Gases	H_2S	Cl_2	NH_3	LPG	CH_3OH	C_2H_5OH
Selectivity coefficient (K)	4.8	12.3	17.1	8.4	17.4	18.3

Signature Not Verified
SHAHAJAHAN
MEHABUB MANER
Document Certified

ACCEPTED MANUSCRIPT

ACCEPTED MANUSCRIPT

Figure: 1

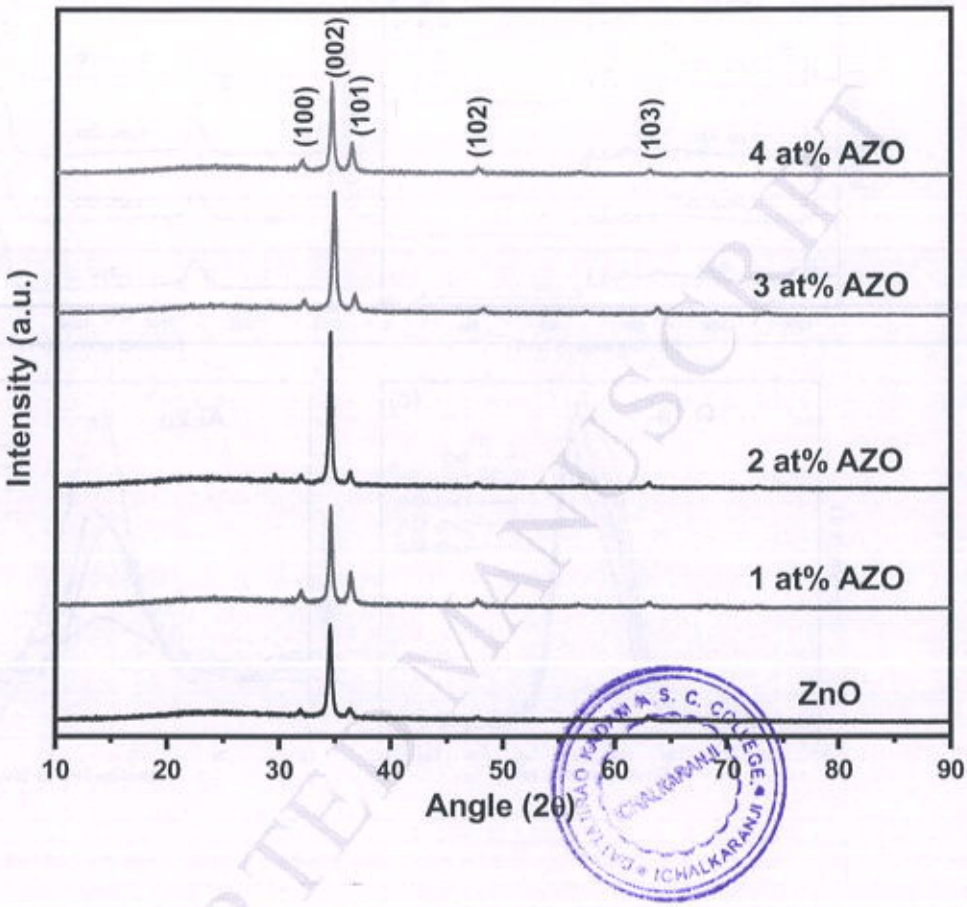

ACCEPTED MANUSCRIPT

Signature Not Verified
SHAHAJAHAN
MEHABUB MANER
Document Certified

ACCEPTED MANUSCRIPT

Figure: 2

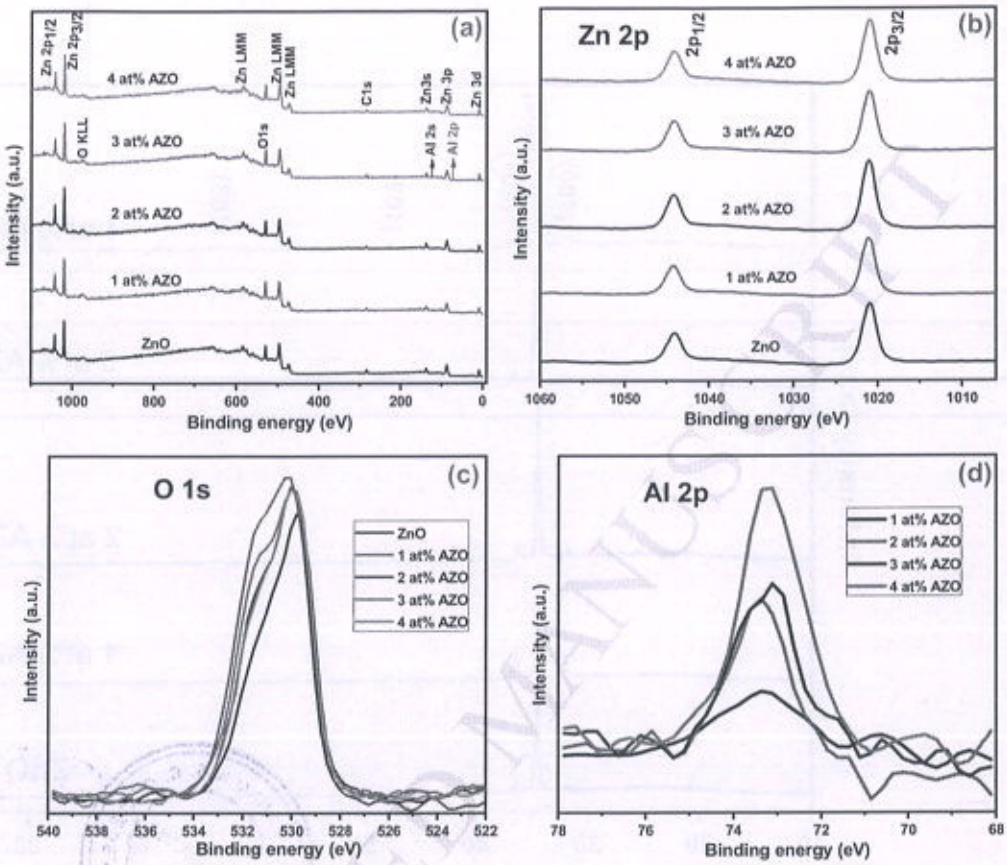

Signature Not Verified
SHAHAJAHAN
MEHABUB MANER
Document Certified

ACCEPTED MANUSCRIPT

Figure: 3

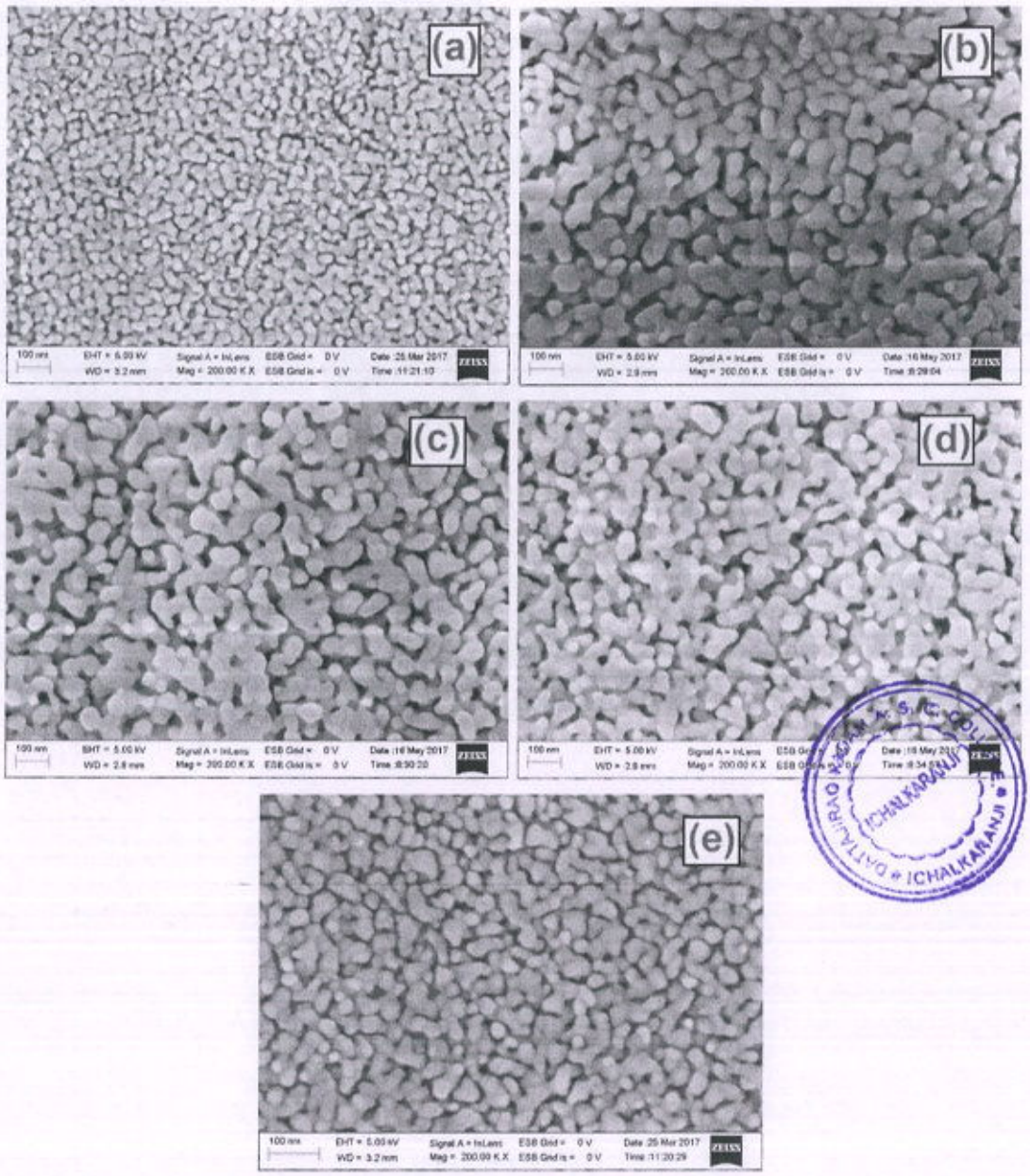

Signature Not Verified
SHAHAJAHAN
MEHABUB MANER
Document Certified

Figure: 4

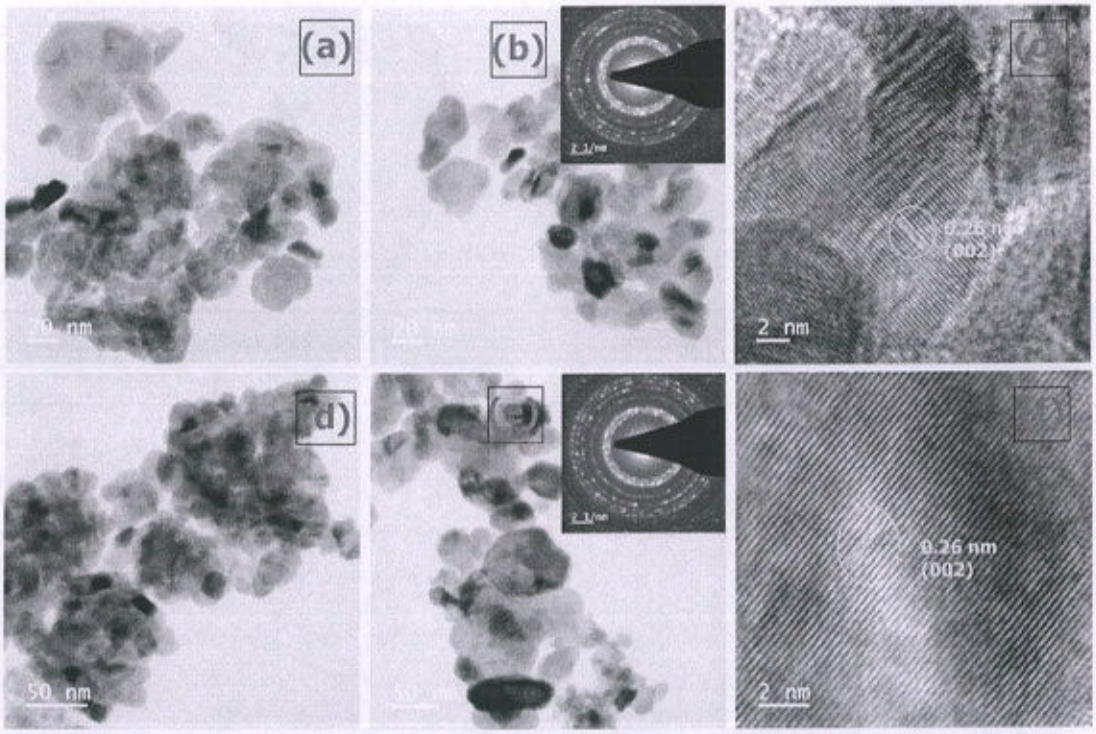

ACCEPTED MANUSCRIPT

Signature Not Verified
SHAHAJAHAN
MEHABUB MANER
Document Certified

ACCEPTED MANUSCRIPT

Figure: 5

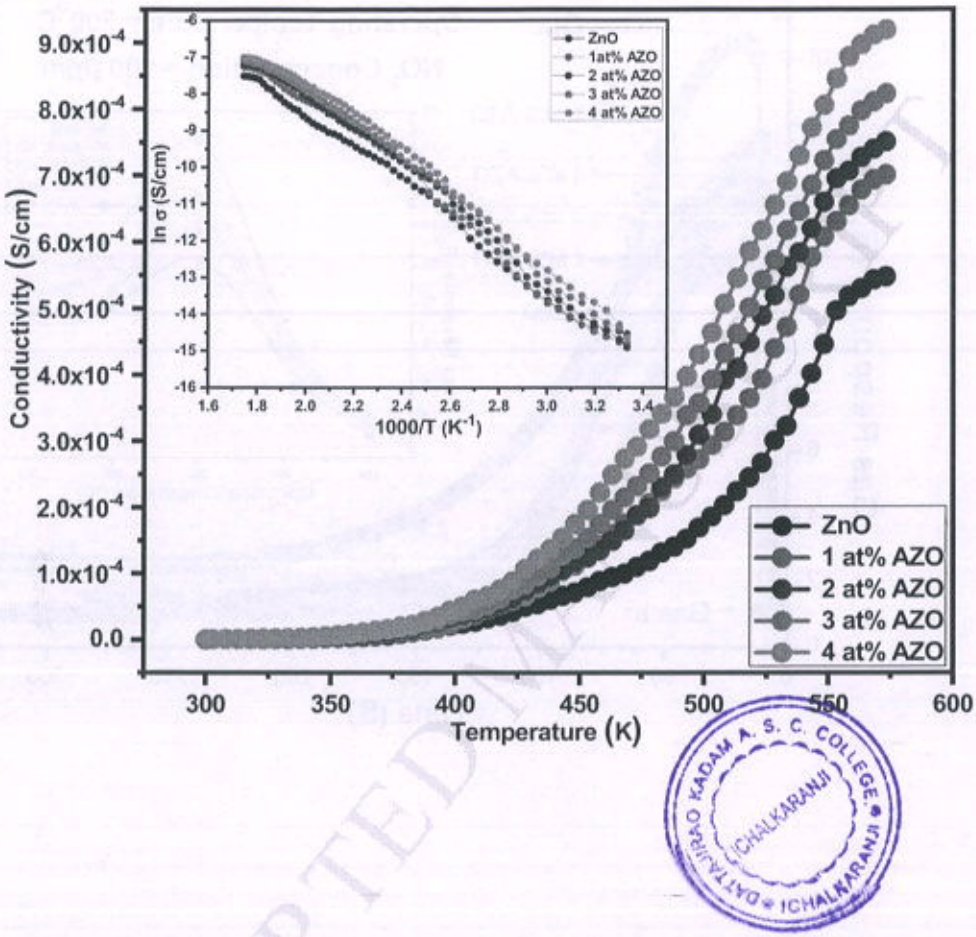

DATTARAO KADAM A. S. C. COLLEGE ICHALKARANJI

Signature Not Verified
SHAHAJAHAN MEHABUB MANER
Document Certified

ACCEPTED MANUSCRIPT

Figure: 6

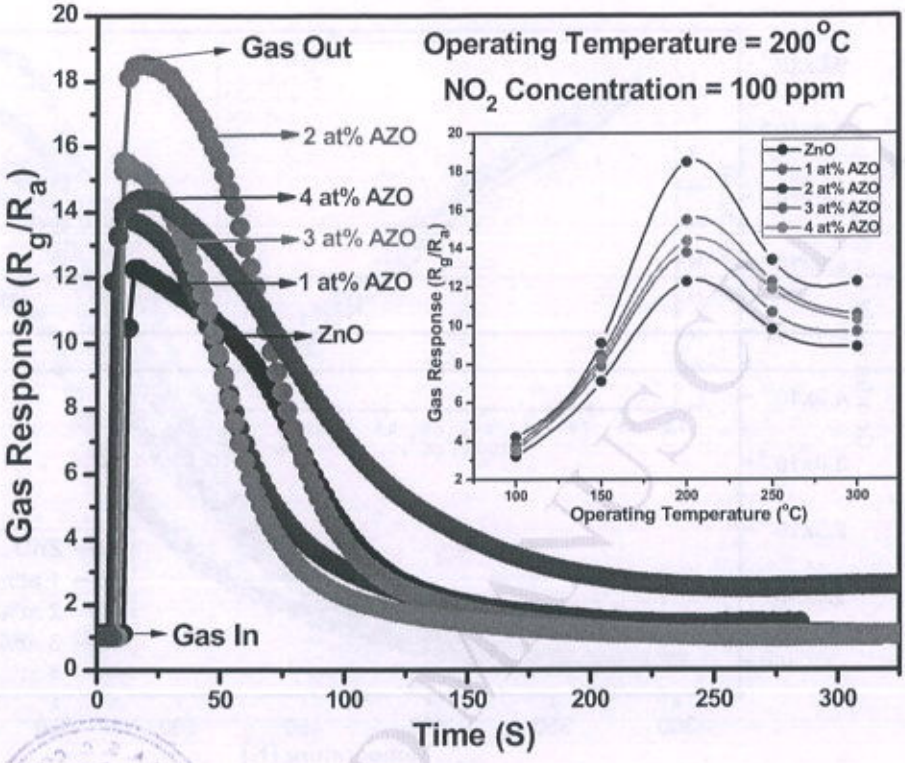

ACCEPTED MANUSCRIPT

Signature Not Verified
SHAHAJAHAN MEHABUB MANER
Document Certified

ACCEPTED MANUSCRIPT

Figure: 7

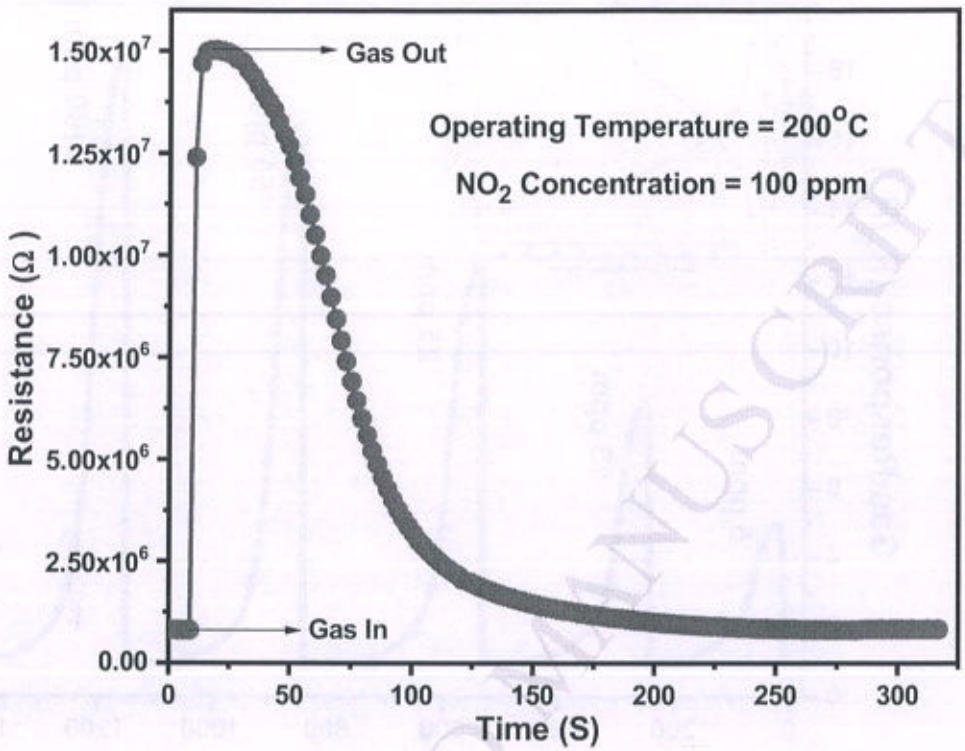

DATTAJIRAO KADAM A. S. C. COLLEGE ICHALKARANJI ICHALKARANJI

Signature Not Verified
SHAHAJAHAN
MEHABUB MANER
Document Certified

ACCEPTED MANUSCRIPT

Figure: 8

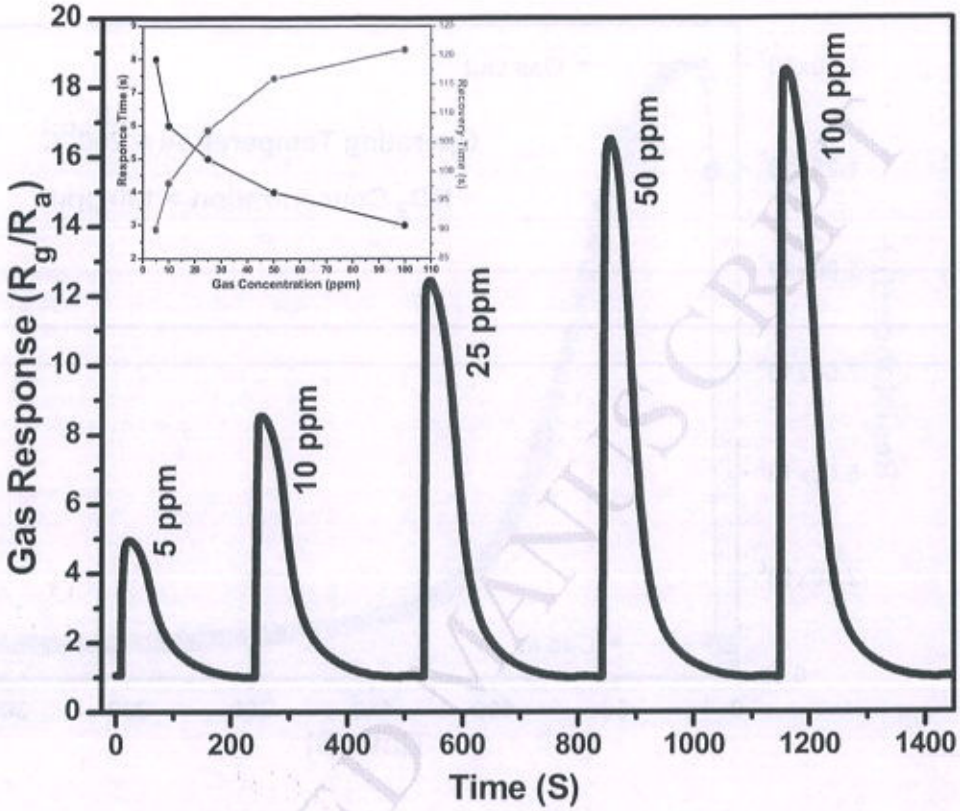

DATTAJIRAO KADAM A. S. C. COLLEGE ICHALKARANJI

Signature Not Verified
SHAHAJAHAN
MEHABUB MANER
Document Certified

ACCEPTED MANUSCRIPT

Figure: 9

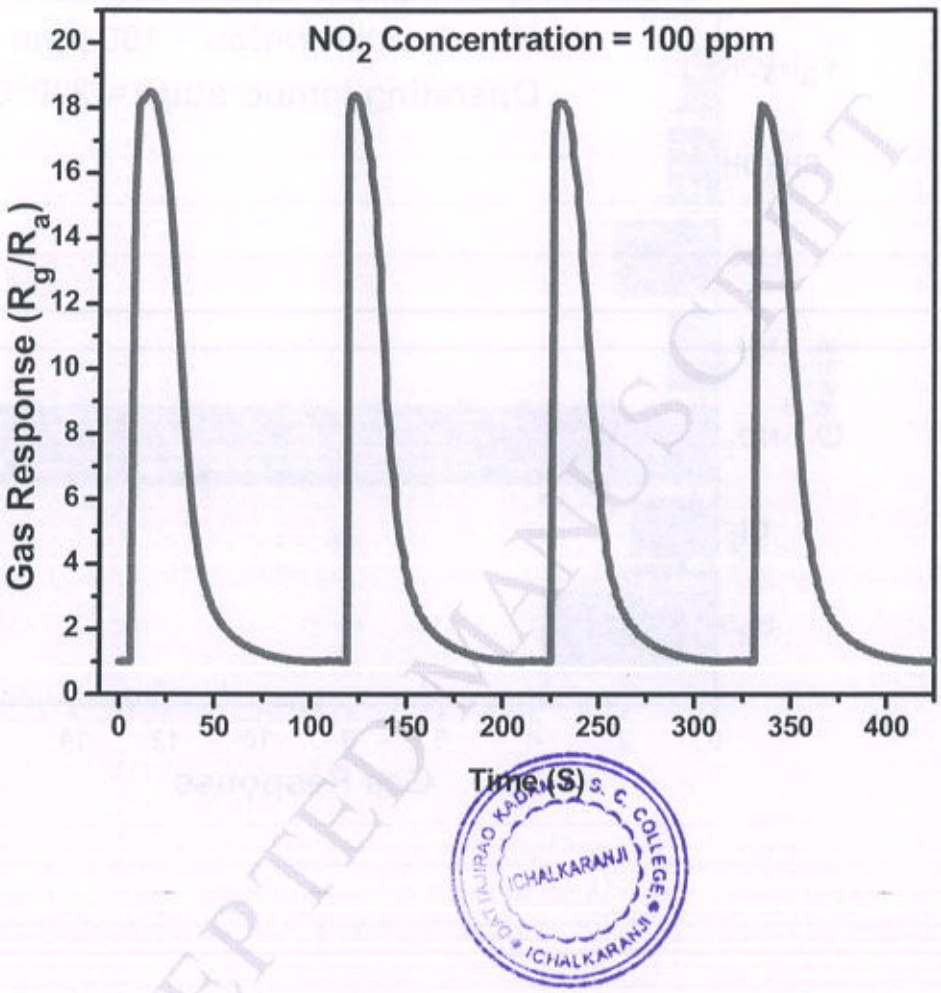

ACCEPTED MANUSCRIPT

Signature Not Verified
SHAHAJAHAN MEHABUB MANER
Document Certified

ACCEPTED MANUSCRIPT

Figure: 10

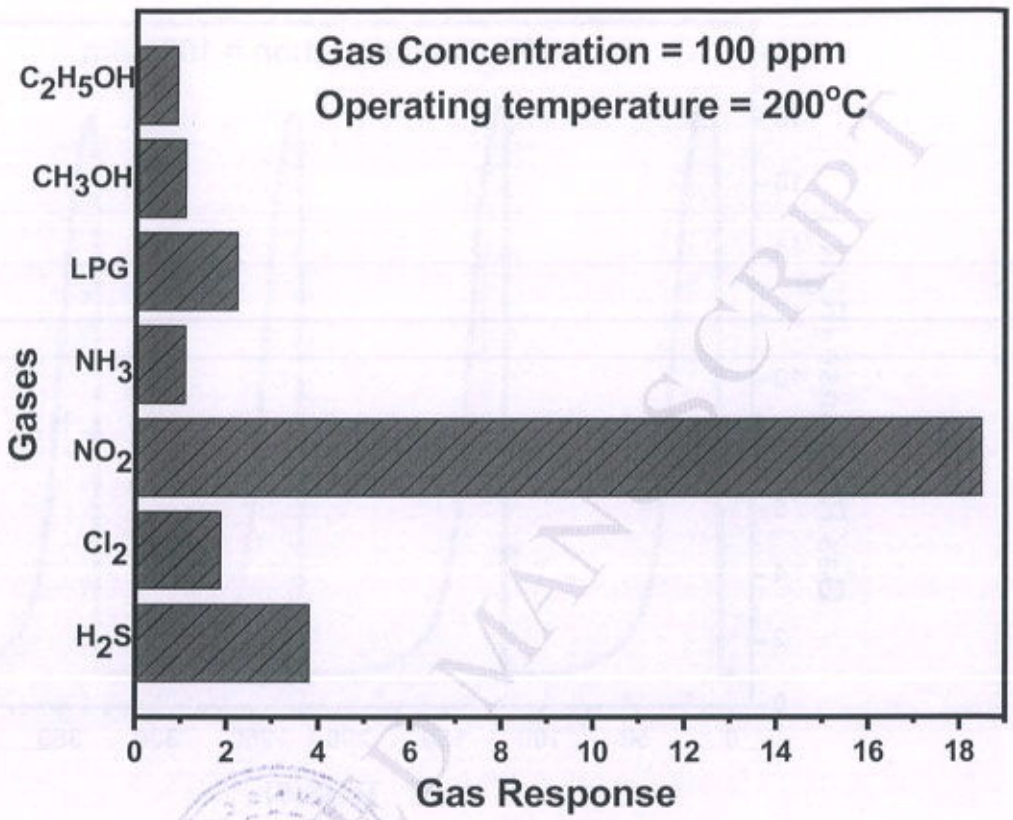

DATTAJIRAO KADAM A. S. C. COLLEGE, ICHALKARANJI
ICHALKARANJI

Signature Not Verified
SHAHAJAHAN
MEHABUB MANER
Document Certified

ACCEPTED MANUSCRIPT

Research highlights

- Effect of Al doping on NO_2 gas sensing properties of ZnO thin films is studied.
- XPS study reveals the substitution of Al atoms into ZnO lattice.
- The 2 at% AZO thin film detects 5 ppm NO_2 concentration at 200°C.

ACCEPTED MANUSCRIPT

Signature Not Verified
SHAHAJAHAN
MEHABUB MANER
Document Certified

AAYUSHI INTERNATIONAL INTERDISCIPLINARY RESEARCH JOURNAL
(Peer Reviewed and Indexed Journal)

Special Issue No : 49 | Impact Factor : 5.707 | ISSN : 2349-638x

International Conference

On

"Advanced and Innovative Practices in Commerce & Management, Science & Technology, Humanities, Languages and Their Role in Achieving the Exponential Growth"

Date : 16th February 2019

Organised by

Shri Narayanrao Babasaheb Education Society's

SHRI VENKATESH MAHAVIDYALAYA, ICHALKARANJI

In collaboration with

Shivaji University Commerce and Management Teachers Association (SUCOMATA)

and

BVDU's Institute of Management and Entrepreneurship Development, (IMED) Pune

Editorial Board

Chairman : Prin. Dr. Vijay Annaso Mane
Editor-in-chief : Dr. Naushad Makbool Mujawar
Co-editor : Mrs. Sunita Hansraj Ambawade

VOLUME 2

Web : www.venkateshcollege.com
Mail Id : mshrivenkatesh@yahoo.com

Signature Not Verified
SHAHAJAHAN MEHABUB MANER
Document Certified

STUDY OF BIODIVERSIY AND SURVEY OF SOME MEDICINAL PLANTS ON NARANDE HILLS, HATKANGALE (KOLHAPUR)

Mr. S. T. Ingle
Dept. of Botany, D. K. A. S. C. College, Ichalkaranji, Dist. - Kolhapur -416115 (M.S.)
Email: subhashingle529@gmail.com

ABSTRACT

An attempt has been made for survey and Biodiversity of medicinal Plants in religious holy pla "Narande" hills, it is famous for "Nagoba" temple. It is located 3 Kim. Away from Hatkangale Tahsil. These have great significance in utilization of wild resources of medicinal plants. During the study of biodiversit survey, thirty plants assessed by Quadrate method. These are found to have Medicinal values as remedy for diff health problem by local people. It is revealed that, these wild resources (medicinal plants) are utilized by local p as per their needs but not exploited on a large scale.

Keywords: *Biodiversity, Narande hills, medicinal plants, Assessment.*

Introduction

It is the fact that over 70-80% of the world population depends on the crude plant drugs to get rid of their health aliments. An Indian material Medica includes about 2000 drugs of natural origin derived from different traditional systems and folklore medicines[1] while in modern medicines over 130 drugs originally extracted from higher plants. In last few decades, new trends of 'Herbal Drugs' from medicinal plants has becoming more prominently apparent[2]. Now days it has been estimated that the present global market is going at the rate of 20% annually[1]. Here the concept of Ayurveda begin and flourish between 2500-500 BC in India. The use of medicinal plants were documented in old literature half majority of them are found in *Rig-Veda* and *Athervveda* and also in *Charakasanhita* (900 BC), *Sushruta Sanhita* (600 BC) and *Ashtang Hridaya* (700 AD). Thus Ayurveda now has become scientifically organized.

India is a store house of medicinal plants and there are some 1250 Indian medicinal plants[4]. Survey of Kolhapur district shows 600 plant species of some therapeutic value. Out of them some important medicinal plants are found in the forest *Narande* hills. *Narande* hills are a holy place for Hindu temple in hilly region of Hatkangale Tahsil. It is situated at 16'45N, 74'22' E and at altitude 773 m. The vegetati dry deciduous[5]. Narande is the part and parc Sahayadri ranges. The biodiversity of Nar hills show different medicinal plants in the of herbs, shrubs, trees and climbers.

The common medicinal plants are ass in this area like as *Plumbago zeylanic Gloriosa sauperba* L., *Discoriea bulbiflor Borrhavia diffusa* L., *Vitex negundo, La procumbens, Lantana camara* L., *Termi arjuna, Clerodendrum serratum, Gi tiliaefolia* etc.

Material and Method

The assessment of medicinal plants st with the help of a Quadrat method. The sha Quadrat is usually square. The size of Qu varies with the type of vegetation to be stu The Quadrate of 10 m by 10 m size ar randomly at three differ rent places and sp are recorded with their number in each. The species are identified by using sta literature[6]. The abundance, density, freq and frequency percentage of each speci determined by using the standard methods. use the Standard methods[8]. The herb specimens are maintained in the c department by following routine herb techniques.

Signature Not Verified
SHAHAJAHAN MEHABUB MANER
Document Certified

tion

Table1. Assessment of Medicinal plants by Quadrate analysis

me of plants ecies	Quadrate 1	2	3	Total No. of species in all Qua.	Total no. of Qua. Studied	No. of Qua. in which species occur	Abundance	Density	Frequency %	Frequency class
gacea mollis edu	02	05	03	10	03	03	3.33	3.33	100	E
ssia auriculata L.	05	-	07	12	03	02	4	6	66	D
alvastrum cuspidutum (R. . Gray.	03	02	06	11	03	03	3.66	3.66	100	E
ommelina galensis L.	08	06	10	24	03	03	8.0	8	100	E
itex negundo L.	03	15	05	23	03	03	7.66	7.66	100	E
calypha indica L.	14	15	17	46	03	03	15.33	15.33	100	E
evandula ermanni Benth.	11	24	13	48	03	03	16.0	16.0	100	E
ribulus terrestris L.	26	37	29	94	03	03	31.33	31.33	100	E
[illegible] ucronata Wild.	02	14	17	33	03	03	11.0	11.0	100	E
avandula ermanni Benth.	11	24	13	48	03	03	16.0	16.00	100	D
yanotis axillaris .) D. Don.	13	07	09	29	03	03	9.66	9.66	100	E
permacoce hispida cutnon	19	27	32	79	03	03	26.33	26.33	100	E
ungia crenata ndres	02	26	08	36	03	03	12	12	100	E
hrbia hirta L.	21	17	33	73	03	03	24.33	24.33	100	E
ursera penicillata Sesse & Moc ex C.)	03	05	04	12	03	03	4	4	100	E
leusine indica (L.)	20	23	18	61	03	03	20.33	20.33	100	E
apicum mericanum L.	03	---	07	10	03	02	3.33	5.66	100	E
olygala arvensis Willd.	02	---	07	09	03	02	3.0	3.0	100	E
canthospermum ispidatum L.	08	11	16	35	03	03	11.66	11.66	100	E
antaena camera L.	06	11	10	27	03	03	9.0	9.0	100	E
Bidens pilosa uct.non .L.	133	106	95	334	03	03	111.33	111.33	100	E
Evolvulus alsinoides L.	06	05	07	18	03	03	6.0	6.0	100	E
Trichodesma amplexicaule Roth.	07	05	03	15	03	03	5.0	5.0	100	E
Echinops echinatus Roxb.	15	06	---	21	03	02	7.0	10.5	66.66	E

Signature Not Verified
SHAHAJAHAN MEHABUB MANER
Document Certified

Signature Not Verified
SHAHAJAHAN
MEHABUB MANER
Document Certified

jpht

Journal of Postharvest Technology
2018, 06(4): 75-81
http://www.jpht.info

RESEARCH ARTICLE

Texture profile analysis of Sonaka and Thompson seedless raisins

Vijaykumar A. Patil and Vishal V. Naik*

Post-graduate Department of Botany, D. K. A. S. C. College, Ichalkaranji, Tal. Hatkanangale, Dist. Kolhapur (MS), India- 416 115. Affiliated to Shivaji University, Kolhapur- 416 004.

Received: 20.08.2018 Accepted: 15.09.2018

ABSTRACT

Texture Profile Analysis (TPA) is a well developed and reliable method for measuring firmness of fruits and dehydrated products. In the present investigation, an attempt has been made to study texture profile of raisins of Sonaka and Thompson seedless treated with $MgCO_3$, $K2CO_3$, $CaCO_3$ and Sulphur and coated with Zein protein. Results indicated that hardness of raisins of both varieties was increased due to Zein protein coating and sulphur treatment. The adhesiveness of sulphur treated and Zein coated raisins was reduced in Thompson seedless variety. The raisins of Sonaka and Thompson seedless variety had the least cohesiveness under sulphur, Zein protein coating indicated that both treatments improved durability of and deformation of raisins during post harvest storage. From these results it is concluded that application of sulphur and Zein protein coating on raisins of Sonaka and Thompson seedless is beneficial for maintenance of overall texture of raisins during storage and transport.

Keywords: Raisins, Sonaka, Sulphur, Thompson seedless, TPA, Zein protein

Citation: Patil, V.A. and Naik,V.N. 2018. Texture profile analysis of sonaka and thompson seedless raisins. *Journal of Postharvest Technology*, 6(4): 75-81.

INTRODUCTION

Grape (*Vitis vinifera* L.) belonging to family Vitaceae is a commercially important fruit crop of India. Grapes are eaten as raw or they can be used for making wine, raisins, jam, and jelly, which are very nutritious and rich source of minerals like potassium, phosphorus, calcium, magnesium and other micronutrients and different vitamins. The dried grapes, commonly known as raisins, have a great importance in economy of the country and considered as one of the nutritious most popular dry fruits in the world. Raisins are dried fruits of certain varieties of grapevines with a high content of sugar and solid flash (Khair and Shah, 2005). The important raisin grape varieties are Thompson seedless and their selections like Tas-A-Ganesh, Sonaka and Manikchaman. The increased production of table grapes has a great potential to produce raisins with minimum losses of fresh fruits (Telis et al., 2004).

Texture profile analyses (TPA) is a well developed and reliable method for measuring firmness of fruits and dehydrated products (Harker et al., 2006) and has been utilized for measuring the physical properties of plant tissue (Bourne, 2002 and Roudot, 2006) mostly from wide range of food and vegetables (Chang et al., 2012, Kulamarva et al., 2009 and Cardoso et al., 2009). TPA provides sensory signals to consumers (Civille, 2011) and thus it stands as one of the measures in the food chain used to estimate the quality of different cultivars at technological ripeness and during storage (Paoletti et al., 1993 and Johnston et al., 2000).

* *For correspondence:* V. V. Naik (Email: purslanevvn@gmail.com)

Signature Not Verified
SHAHAJAHAN MEHABUB MANER
Document Certified

In the present investigation, an attempt has been made to study texture profile of raisins of Sonaka and Thompson seedless treated with $MgCO_3$, K_2CO_3, $CaCO_3$ and Sulphur and coated with Zein protein. Present study may be beneficial to farmers for post harvest storage of raisins

MATERIALS AND METHODS

Raw Martial

The grapes of two varieties viz. Sonaka and Thompson seedless were harvested at Malgaon (Tahsil- Miraj, District- Sangli, Maharashtra, India) when they were fully ripened, having sugar percentage more than 21° brix. It required nearly 130 to 150 days for harvesting the grapes for raisin preparation. For raisin preparation, grapes were harvested early in the morning and treated with different chemicals as follows:

$MgCO_3$, $CaCO_3$ and K_2CO_3 were taken in different concentrations of 10, 15, 20, 22, 23, 24, 25, 26 and 30 mg/liter in buckets and after stirring and dissolving the chemicals, 18 ml olive oil were mixed. A dipping oil ethyl oleate was kept constant 18 ml/liter of water in all pre-treatment chemical samples.

Texture profile analysis (TPA)

Texture Profile Analysis was carried out to determine the quality of raisins pretreated with different treatments. Single treated raisin had been used for the texture profile analysis. For the estimation of texture quality, instrument called TA-XT2 Plus, Texture Analyser, made by Stable Micro System, London had been utilized. The settings used for the analysis was: Pre Test Speed- 1.00 mm/sec, Test speed - 5.00 mm/sec, Post Test Speed- 5.00 mm/sec, Target Mode- Strain at 40%, Test Time- 5 sec, Probe - P/75 mm Compression Platen and Data Acquisition Rate: 200 pps (parts per sec).

RESULTS AND DISCUSSION

Texture Profile Analysis

The texture profile analysis of Sonaka and Thompson seedless raisins is shown in the Table 1. It is noticed that the hardness of Sonaka seedless raisin is less than that of Thompson seedless raisins treated with $MgCO_3$, K_2CO_3 and $CaCO_3$. While, the raisins treated with Sulphur and coated with Zein protein shows remarkable increase in the hardness of Sonaka than the Thompson seedless raisins. It is also noticed that the hardness of, Sulphur and coated with Zein protein raisins is significantly increased than uncoated raisins.

It is clear from Table 1 that the adhesiveness of, Sulphur and Zein protein coated raisins of Thompson seedless variety has been significantly decreased than the treated control raisins. While, in case of raisins of Sonaka variety adhesiveness is slightly altered. The springiness of raisins of Sonaka and Thompson seedless variety is almost similar and due to the Sulphur and Zein protein coating the springiness of raisins remains unchanged or slightly altered (Table 1). The cohesiveness of raisins of Sonaka and Thompson seedless variety is significantly decreased in, Sulphur and Zein protein coated raisins than the controlled raisins (Table 1).

It is evident from Table 2 that the gumminess of raisins of Thompson seedless variety is slightly decreased due to Sulphur and Zein protein coating treatment than the control, while, the raisins of Sonaka seedless variety shows increase in the gumminess due to pretreatment with , Sulphur and Zein protein coated than the control raisins. The chewiness of both the varieties of Sonaka and Thomson seedless raisins has been elevated due to, Sulphur and Zein protein coating pretreatment than the

Signature Not Verified
SHAHAJAHAN MEHABUB MANER
Document Certified

control pretreatment (Table 1) while the resilience of Sonaka and Thompson seedless variety raisins is slightly decreased due to the pretreatment of, Sulphur and Zein protein coating than the control pretreatment (Table 1).

Table 1. Texture Profile Analysis of raisins of Sonaka and Thompson seedless under different chemical treatments.

Test ID	Force 1 g	Area-FT 1:2 g sec	Time-diff. 1:2 sec	Area-FT 1:3 g sec	Area-FT 2:3 g sec	Area-FT 4:6 g sec	Time-diff. 4:5 sec	Hardness g	Adhesive-ness g.sec	Springi-ness	Cohesive-ness	Gummi-ness	Chewi-iness	Resili ence
TPA 1	1222.38	150.81	0.661	201.44	50.63	141.31	0.594	1363.1	-0.64	0.89	0.7	955.02	856.40	0.33
S.D.	273.20	38.805	0.096	53.03	15.07	39.469	0.1	305.96	0.29	0.03	0.02	227.43	214.90	0.036
C. V	22.35	25.731	14.47	26.32	29.78	27.93	16.88	22.446	-45.02	4.12	3.69	23.815	25.09	10.58
TPA 2	454.36	60.79	0.648	79.92	19.12	57.61	0.734	504.27	-0.147	1.14	0.72	368.18	527.6	0.29
S.D.	388.50	35.285	0.034	49.163	14.42	37.013	0.25	422.29	-	0.44	0.074	328.89	669.44	0.062
C. V	85.505	58.038	5.218	61.512	75.43	64.24	34.11	83.742	-	38.63	10.18	89.32	126.86	20.66
TPA 3	1153.6	157.97	0.523	196.54	38.56	130.40	0.409	1281.1	-0.46	0.78	0.66	850.51	664.07	0.244
S.D.	208.82	36.27	0.014	44.852	9.012	26.084	0.023	241.09	0.088	0.028	0.026	133.97	99.56	0.023
C. V	18.103	22.95	2.762	22.8	23.36	20.03	5.594	18.82	-19.172	3.55	3.904	15.753	14.99	9.328
TPA 4	874.57	155.76	0.558	187.58	31.82	122.04	0.43	989.26	-0.163	0.77	0.65	643.88	497.15	0.205
S.D.	40.33	7.157	0.049	4.807	2.405	7.85	0.028	55.983	0.172	0.04	0.058	56.49	43.23	0.026
C. V.	4.612	4.595	8.863	2.562	7.557	6.43	6.578	5.659	-105.93	5.15	8.846	8.775	8.69	12.541
TPA 5	1320.58	265.66	0.608	317.40	51.73	146.83	0.436	1655.8	-0.33	0.72	0.54	786.19	548.24	0.213
S.D.	646.24	187.20	0.068	212.94	26.51	49.65	0.084	955.94	0.198	0.122	0.16	261.22	149.2	0.045
C. V.	48.93	70.46	11.25	67.091	51.24	33.99	19.233	57.733	-58.54	16.97	29.46	33.22	27.21	20.975
TPA 6	629.66	113.59	0.631	145.46	31.87	100.73	1.121	701.91	-0.173	1.74	0.706	483.33	768.06	0.283
S.D.	252.57	44.42	0.073	55.73	11.47	32.11	1.074	290.04	-	1.61	0.07	163.48	591.2	0.018
C. V	40.11	39.10	11.63	38.312	36.06	31.88	95.748	41.322	-	92.59	9.99	33.823	76.97	6.432
TPA 7	1313.93	292.49	0.718	349.03	56.54	199.86	0.548	1513.8	-0.18	0.76	0.58	891.79	685.53	0.207
S.D.	119.01	76.04	0.051	71.737	4.445	11.98	0.028	99.299	0.23	0.031	0.104	198.08	181.15	0.079
C. V	9.058	26	7.144	20.553	7.862	5.99	5.185	6.559	-127.12	4.046	17.75	22.212	26.42	38.173
TPA 8	1652.48	346.35	0.596	413.26	66.91	230.47	0.469	1957.02	-0.17	0.78	0.55	1094.42	854.17	0.192
S.D.	435.65	63.70	0.05	79.741	16.18	58.26	0.046	503.972	0.13	0.033	0.038	342.64	243.83	0.013
C. V	26.36	18.39	8.439	19.295	24.18	25.28	9.753	25.752	-80.44	4.24	6.91	31.308	28.54	6.853

S.D. – Standard Deviation; **C.V.** – Coefficient of Variance. **TPA-1**: Thompson seedless treated with $MgCO_3$; **TPA-2**: Sonaka seedless treated with $MgCO_3$; **TPA-3**: Thompson seedless treated with K_2CO_3; **TPA-4**: Sonaka seedless treated with K_2CO_3; **TPA-5:** Thompson seedless treated with $CaCO_3$; **TPA-6:** Sonaka seedless treated with $CaCO_3$; **TPA-7**: Thompson seedless treated with K_2CO_3+Sulpher Fumigated and coated; **TPA-8:** Sonaka seedless treated with K_2CO_3+Sulpher Fumigated and coated.

According to Civille (2011), the mechanical properties viz. hardness, cohesiveness, crispness, crunchiness and denseness of food are easy indicators of a product's freshness and wholesomeness. Texture profile parameters determined were as follows - firmness, cohesiveness, adhesiveness and chewiness (Besbes et al., 2009). In this respect, there has been a great interest in developing methods to predict and control the texture of the food, particularly in regard to the effects of processing like drying. According to Alvarez et al. (2002), it involves the puncture test method that is more linked to the skin texture indicating that fruit skin plays a great part in the overall firmness (Grotte et al., 2001). The analysis of the instrumental texture profile

Signature Not Verified
SHAHAJAHAN MEHABUBMANER
Document Certified

analysis (TPA) is one of the methods for determining the texture of food by simulation or imitation of repeated biting or chewing food (Almeida, 2013). Instrumental TPA or double compression test was based on the analysis of each intact berry, which was compressed twice with a 25% deformation 25 apart, in reciprocating motion imitating the action of the jaw (Maury et al., 2009). Textural properties of whole berry depend on different characteristics like cell - wall composition, cell structure and pulp turgescence, and therefore this mechanical test can be useful to follow grape ripening (Moigne et al., 2008).

Letaief et al. (2008) designated berry chewiness to be a dominant texture parameter in differentiating Italian varieties of grape. A significant varietal effect was observed for berry hardness, gumminess, springiness, chewiness and resilience on Merenzao varieties (Segade et al., 2011). Mechanical texture parameters were able to show the differences between grapes with different ripening levels (Maury et al., 2009). Marsilio et al. (2000) speculated that the textural properties as well as the appearance and flavor are the most influential organoleptic attributes for quality, which indicates the acceptability of food by consumers. The complex interactions between different components of the food resulted in the development of texture and the changes related with the texture of food during food processing are due to the structural changes in the cell (Marsilio et al., 2000).

According to Caine et al. (2003), hardness is the force required to compress a food between the teeth or between the tongue and mouth, i.e. the force required to cause deformation, while the elasticity is the ability to regain shape after compression, and measures the speed of return to the initial state after removal of the force which caused the deformation. They noticed that the elasticity value decreases with increasing temperature. The raisins obtained by solar drying are less elastic than those obtained by drying in a ventilated oven at 50°C and in turn less elastic than the grapes dried at 60°C. The results in the present study are in agreement with those obtained by Caine et al. (2003). The cohesiveness represents the internal forces in the food, and maintains the sample cohesive (Caine et al., 2003). They found that the results for the samples from the solar greenhouse and from the ventilated chamber at 50°C were similar, while the grapes dried at 60°C were less cohesive. Resiliency is the strain energy per unit volume to a limit of proportionality, i.e. the energy used when applying a force to a material without to occurring rupture, with or without any residual strain (Caine et al., 2003). The chewiness measures the energy required to disintegrate a food as to be swallowed (Caine et al., 2003), and these results are derived directly from the fact that these grapes have a higher hardness than the others. The mechanical characteristic of texture, which is commonly used to describe the rheological behavior of biological materials, is the Firmness (or hardness) and is generally defined as the maximum force required to achieve a specific strain in compression, puncture and cut tests (Peleg, 2006). The fact that the greater force in the longitudinal direction may be due to the location of the polysaccharide chains of the cell wall with respect to the load application as suggested by Mayor et al. (2007). The several investigators (Van Linden,V. 2007; Toivonen and Brummell, 2008 and Goulao and Oliveira, 2008) have reported as fruit ripeness that progresses, water loss occurs, which is associated with a loss of turgor of the cells, a decrease in adhesion between cells and changes in cell wall polysaccharides,.

In the present investigation the various parameters of texture were positively influenced due to pretreatments of chemicals and coating. The hardness of Zein protein coated raisins was increased than that of control. Thus, the increased hardness of raisins will improve the marked quality and durability of raisins due to the Zein coating and sulphur treatment.

The adhesiveness of sulphur treated and Zein coated raisins was reduced in the raisins of Thompson seedless variety. The decreased or low adhesiveness is an important property of dehydrated fruit which maintains the shelf life of raisins during post harvest storage of raisins thus the application of Zein coating is found to be beneficial for maintaining this textural property of this raisins.

Signature Not Verified
SHAHAJAHAN
MEHABUB MANER
Document Certified

The springiness of raisins of Sonaka and Thompson seedless variety was slightly altered or almost unchanged which indicate that the stability of raisins due to various pretreatment results in the better quality of raisins. Thus the maintenance of springiness thought, the treatment results in the maintenance of its normal size after compression pressure during the storage and transport. This will improve the market quality and acceptability of raisins by consumer.

The raisins of Sonaka and Thompson seedless variety had the least cohesiveness of sulphur, Zein protein coated, raisins which was slightly lowered thus the maintenance of less cohesiveness during the course of its storage indicates its maintenance of texture after second deformation. Thus, it can improve the overall durability and deformation of raisins during post harvest storage.

The slight change in gumminess of Thompson seedless raisins than in Sonaka seedless raisins was noticed which indicate that the elevation in gumminess of semisolid raisins is related to its hardness hence these changes in gumminess is correlated with the hardness of these to raisins varieties. Thus, this will definitely improves the overall storage and durability of this perishable product. The chewiness is property of solid product calculated with springiness and gumminess thus the slight changes in chewiness of raisins of Sonaka and Thompson seedless variety indicates positive influence of pretreatment on quality and consumer acceptability of raisins.

The resilience is measure of the single peak compression obtained after withdraw of first compression. In the present study, less resilience of raisins in these two verities was noticed which will be found beneficial for maintaince of overall texture of the raisins during storage and transport.

CONCLUSION

Considering the sensory evaluation, nutritive value and physio-chemical changes during storage the treatment combination T_2 that is 1: 1.25 pulp to sugar ratio of strawberry jam could be selected for commercial processing. After 6 months of storage under room temperature, the quality and the nutritional changes of strawberry jam was found satisfactory. For this regards it was concluded that strawberry jam may be stored up to 6 months at room temperature.

REFERENCES

Almeida, I. C. 2013. Desenvolvimento de produtos de uva passa a partir da uva de mesa da variedade crimson. Dissertação do Mestrado em Qualidade e Tecnologia Alimentar. Escola Superior Agrária de Viseu, Viseu.

Alvarez, M. D., Canet, W. and Lopez, M. E. 2002. Influence of deformation rate and degree of compression on textural parameters of potato and apple tissues in texture profile analysis. Eur. Food Res. Technol., 215: 13–20.

Besbes, S., Drira, L., Blecker, C., Deroanne, C. and Attia, H. 2009. Adding value to hard date (Phoenix dactylifera L.): compositional, functional and sensory characteristics of date jam. Food Chem. 112: 406–411.

Bourne, M. C. 2002. Food Texture and Viscosity: Concept and Measurement. Second Edition. Academic Press, New York. pp. 400.

Caine, W. R., Aalhus, J. L., Best, D. R., Dugan, M. E. R. and Jeremiah, L. E. 2003. Relationship of texture profile analysis and Warner-Bratzler shear force with sensory characteristics of beef rib steaks. Meat Science, 64: 333-339.

Signature Not Verified
SHAHAJAHAN MEHABUBMANER
Document Certified

Cardoso, C. M. L., Mendes, R. and Nunes, M. L. 2009. Instrumental texture and sensory characteristics of cod frankfurter sausages. Int. J. Food Prop., 12: 625-643.

Chang, H. J., Xu, X. L., Zhou, G. H. and Li, C. B., Huang, M. 2012. Effects of characteristics changes of collagen on meat physicochemical properties of beef Semitendinosus muscle during ultrasonic processing. Food Bioprocess Technol., 5:285–297.

Civille, G. V. 2011. Food Texture: Pleasure and Pain. J. Agric. Food Chem., 59 (5): 1487–1490.

Goulao, L. F. and Oliveira, C. M. 2008. Cell wall modifications during fruit ripening: when a fruit is not the fruit. Trends Food Sci. Tech., 19: 4-25.

Grotte, M., Duprat, F., Loonis, D. and Pietri, E. 2001. Mechanical properties of the skin and the flesh of apples. Int. J. Food Prop. Vigne Vin., 4(1): 149–161.

Harker, F. R., Gunson, F. A. Hallett, I. C. and De Silva, H. N. 2006. Instrumental measurement of apple texture: A comparison of the single-edge notched bend test and the penetrometer. Postharvest Biology and Technology, 39 (2): 185–192.

Johnston, J. W., Hewett, E. W., Banks, N. H., Harker, F. R. and Hertog, M. L. A. T. M. 2000. Physical change in apple texture with fruit temperature: Effects of cultivar and time in storage. Postharvest Biol. Technol., 23: 13–21.

Khair, S. M. and Shah, S. A. 2005. Rapes drying: an indigenous profitable enterprise in Balochistan. J. of Applied Sciences, 5(3): 563-568.

Kulamarvaa, A. G., Soslea V. R. and Vijaya G. S. 2009. Nutritional and Rheological Properties of Sorghum. Int. J. Food Prop. 12(1):55-69.

Letaief, H., Rolle, L., and Gerbi, V. 2008. Mechanical Behavior of Winegrapes under Compression Tests. Am. J. Enol. Vitic., 59(3): 323-329.

Marsilio, V., Lanza, B., Campestre, C. and De Angelis, M. 2000. "Oven-dried table olives: texturalproperties as related to pectic composition". Journal of the Science of Food and Agriculture, 80: 271-1276.

Maury, C., Madieta, E., Le Moigne, M., Mehinagic, E., Siret, R. and Jourjon, F. 2009. Development of a mechanical texture test to evaluate the ripening process of Cabernet Franc grapes. Journal of Texture Studies, 40: 511–535.

Mayor, L., Cunha, R. L. and Sereno, A. M. 2007. Relation between mechanical properties and structural changes during osmotic dehydration of pumpkin. Food Res. Int., 40: 448-460.

Moigne, L. M., Ch, Maury, Bertrand, D. and Jourjon, F. 2008. Sensory and instrumental characterisation of Cabernet Franc grapes according to ripening stages and growing location. Food Quality and Preference, 19: 220–231.

Paoletti, F., Moneta, E., Bertone, A. and Sinesio, F. 1993. Mechanical properties and sensory evaluation of selected apple cultivars. Lebensm.-Wiss. Technol. 26: 264–270.

Peleg, M. 2006. On fundamental issues in texture evaluation and texturization- A view. Food Hydrocoll, 20:405-414.

Roudot, A. C. 2006. Some considerations for a theory of plant tissue mechanics. Sciences des aliments, 26: 409–426.

DATTAJIRAO KADAM TECHNICAL EDUCATION SOCIETY'S COLLEGE ICHALKARANJI

Signature Not Verified
SHAHAJAHAN MEHABUB MANER
Document Certified

Segade, S. R., Vazquez, E. S., Orriols, I., Giacosa, S. and Rolle, L. 2011. Possible use of texture characteristics of winegrapes as markers for zoning and their relationship with anthocyanin extractability index. International Journal of Food Science and Technology. 46: 386–394.

Telis, V. R. N., Lourençon, V. A., Santos, E. M., Borin, I., Gabas, A. L. and Telis-Romero, J. 2004. Drying rates of Rubi grapes as affected by non-conventional chemical pre-treatments. Drying 2004 – Proceedings of the 14th International Drying Symposium (IDS 2004) Sao Paulo, Brazil, vol. C, pp. 1844-1850.

Toivonen, P. M. A. and Brummell, D. A. 2008. Biochemical bases of appearance and texture changes in fresh-cut fruit and vegetables. Review. Postharv. Biol. Tec., 48: 1-14.

Van Linden, V. (2007). Identification of fruit parameters responsible for impact-bruising of tomatoes. Ph.D. thesis. Katholieke Universiteit Leuven, Leuven, Belgium.

Signature Not Verified
SHAHAJAHAN MEHABUB MANER
Document Certified

View publication stats

Rheedea
Vol. 28(1)
49–50
2018
ISSN: 0971-2313
https://dx.doi.org/10.22244/rheedea.2018.28.1.08

Lectotypification of two names in the genus *Ipomoea* (Convolvulaceae)

Shimpale, V.B.[1]*, Kattee Amrapali, V.[1] and Mayur D. Nandikar[2]
[1]Department of Botany, The New College, Kolhapur, Maharashtra – 416 012, India
[2]Naoroji Godrej Centre for Plant Research, 431 Lawkim Campus, Shindewadi,
Post- Shirwal, Satara Dist., Maharashtra – 412 801, India
*E-mail: shimpale@yahoo.com

Abstract

The names *Ipomoea clarkei* Hook.f. and *I. barlerioides* (Choisy) Benth. ex C.B. Clarke are lectotypified.

Keywords: Convolvulaceae, *Ipomoea barlerioides, Ipomoea clarkei,* lectotypification

Introduction

The genus *Ipomoea* L. is one of the dominant genera in the family Convolvulaceae with *c.* 600 species distributed in tropical and warm temperate regions of the world (Mabberley, 2017). About 63 species are known from India (Shimpale *et al.*, 2014). In the course of taxonomic studies on the genus *Ipomoea* in India, it has been found that *I. clarkei* and *I. barlerioides* are yet to be typified. Hence lectotypes are selected according to Art. 9.3 of ICN (Turland *et al.*, 2018).

Ipomoea barlerioides (Choisy) Benth. ex C.B. Clarke in Hook.f., Fl. Brit. India 4: 201. 1883.

Aniseia barlerioides Choisy, Convolv. Orient. 6: 484. 1834.

Lectotype (designated here): INDIA, **Uttar Pradesh,** 17.04.1814, *s.coll.* Wall. Cat. No. 2256.1 [B] (K001115497, digital image!). Syntypes: Sukanagar, 4.5.1810, *Herb Hamilton*, Wall., Numer. List 2256 B: K (K001115496, digital image!); Kumaon, *s.d.* R., *Blinkworth*, Wall. Cat. No. 1382 (K001112984, digital image!); Mysore, *s.d. Buchanan s.n.* (BM000927905, digital image!). Fig. 1

Note: Choisy (1834) within the protologue of *A. barlerioides* cited "(V.S. ex Wall., et H.Br. Mus.) Hab. India (Gorackpur, Sukanagar, Kamaon, Mysore)". The different localities are associated with the Wall., Numer. List 1382 and 2256. The collections from the aforementioned localities are to be considered as syntypes. We have chosen (K001115497) as the lectotype because the specific epithet '*barlerioides*' was first used in Wall., Numer. List 2256.

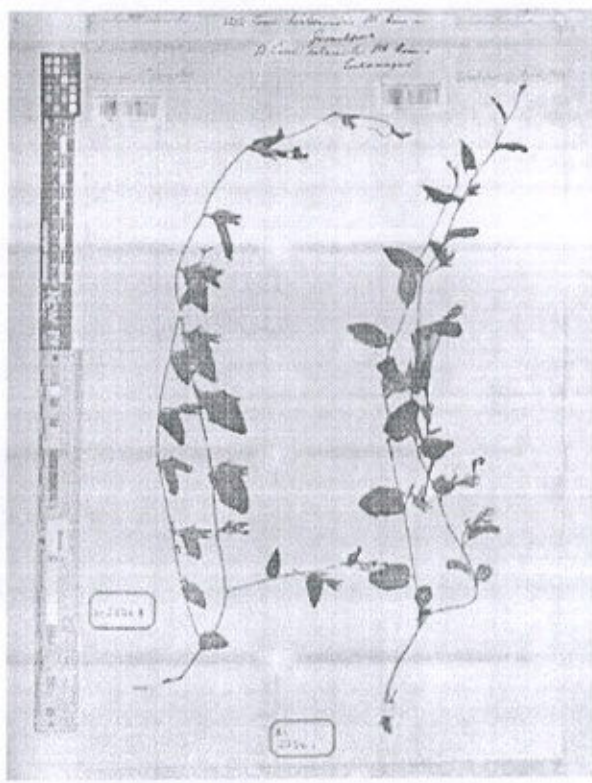

Fig. 1: Lectotype of *Ipomoea barlerioides* (Choisy) Benth. ex C.B. Clarke (Wall., Numer. List 2256: K001115497) [© The Board of Trustees of the Royal Botanic Gardens, Kew. Reproduced with the consent of the Royal Botanic Gardens, Kew].

Signature Not Verified
SHAHAJAHAN
MEHABUBMANER
Document Certified

Ipomoea clarkei Hook.f., Fl. Brit. India 4: 734. 1885.

I. stocksii C.B. Clarke in Hook.f., Fl. Brit. India 4: 207. 1883, non Clarke (1883: 204).

Lectotype (designated here): Malabar, Concan & c. *s.d., Stocks s.n.* (K000830816, digital image!). syntype: Malabar, Concan & c., *s.d., Law s.n.* (K001081777, digital image!). Fig. 2

Note: Clarke (1883) published *I. stocksii* based on the collection of Stocks from Malabar. Clarke (1883) described a different species with the same name based on collections by Stocks, Law & c. from Malabar and Concan. Hooker (1885) considered *I. stocksii* (1883) as a later homonym and provided the new name *I. clarkei*.

There are two relevant specimens at K (K000330816 and K000330817) of which we have designated K000830816 as the lectotype because the sheet has annotation by Clarke and matches with protologue.

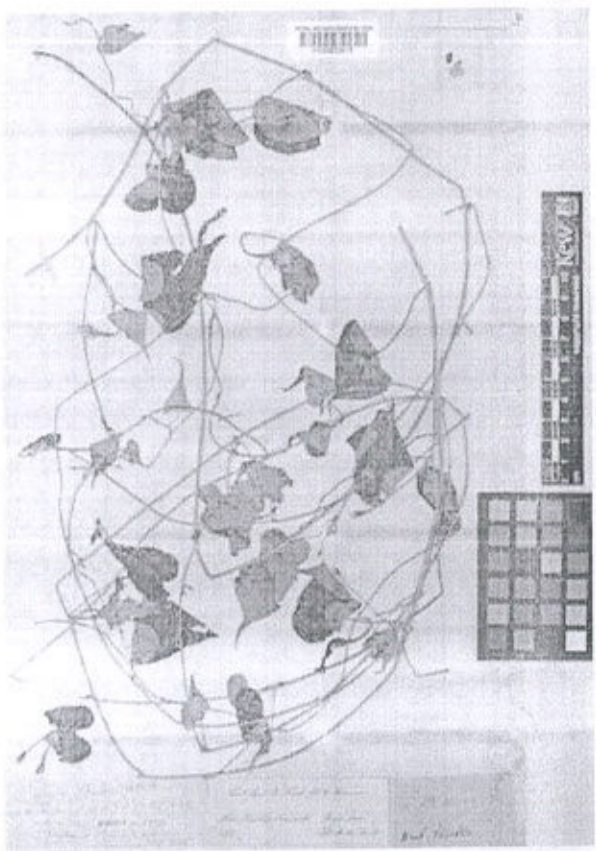

Fig. 2: Lectotype of *Ipomoea clarkei* Hook.f. (Stock *s.n.* K000830816) [© The Board of Trustees of the Royal Botanic Gardens, Kew. Reproduced with the consent of the Royal Botanic Gardens, Kew]

DATTAJIRAO KADAM A.S.C. COLLEGE ICHALKARANJI

Acknowledgements

Authors are thankful to the Principal, The New College, Kolhapur, to the Director, NGCPR, Shirwal for facilities and Board of Trustees of Royal Botanic Garden, Kew, for permission to publish the images of the types.

Literature Cited

Choisy, J.D. 1834. *Convolvulaceae Orientales.* Memoires de la Societè de Physique et d' Histoire Naturelle de Geneve. p. 102.

Clarke, C.B. 1883. Convolvulaceae. In: Hooker, J.D. (Ed.), *Flora of British India.* Vol. 4. L. Reeve & Co., London. p. 201.

Hooker, J.D. 1885. Additions and corrections. In: *Flora of British India.* **Vol. 4.** L. Reeve & Co., London. pp. 733–734.

Mabberley, D.J. 2017. *The Plant - Book: A portable dictionary of plants, their distribution and uses.* Fourth Edition. Cambridge University Press, Cambridge, UK. pp. 466–467.

Shimpale, V.B., Kare, M.A., Londhe, D.K. & A.S. Bhuktar 2014. On the occurrence of *Ipomoea tenuipes* (Convolvulaceae) in India. *Rheedea* 24(2): 117–119.

Turland, N.J., Wiersema, J.H., Barrie, F.R., Greuter, W., Hawksworth, D.L., Herendeen, P. S., Knapp, S., Kusber, W.-H., Li, D.-Z., Marhold, K., May, T.W., McNeill, J., Monro, A.M., Prado, J., Price, M.J. & G.F. Smith (Eds.) **2018.** *International Code of Nomenclature for algae, fungi, and plants (Shenzhen Code).* Regnum Vegetabile 159. Koeltz Botanical Books, Glashütten. DOI https://doi.org/10.12705/Code.2018.

Wallich, N. 1830–1832. *A Numerical list of dried specimens of plants in the East India Company's Museum, collected under the superintendence of Dr. Wallich of the Company's Botanical Garden at Calcutta.* London. p. 67.

Received: 08.05.2017
Revised and Accepted: 10.06.2018

Signature Not Verified
SHAHAJAHAN MEHABUB MANER
Document Certified